RAPID COMMUNICATIONS

PHYSICAL REVIEW E VOLUME 52, NUMBER 3 SEPTEMBER 1995

Interaction of an electron beam with nonuniform gas flow

V. S. Malinovsky and A. V. Vasenkov
Institute of Thermophysics, Russian Academy of Sciences, Novosibirsk, 630090, Russia
(Received 6 March 1995)

A Monte Carlo method was developed to simulate the interaction of an electron beam with a nonuniform gas flow. The model was used to determine the three-dimensional distribution of rates of ionization and excitation of $C\ ^3\Pi_u$ in nitrogen. The results indicate that ionization in a jet occurred much less efficiently than in uniform flow. It was shown that isotropic scattering and no electron beam degradation should be considered when modeling the interaction of a high-energy electron beam with a low density jet.

PACS number(s): 52.20.Fs, 52.40.Mj, 34.80.Gs, 34.80.Dp

I. INTRODUCTION

The knowledge of the electron distribution function (EDF) is of paramount importance in understanding the physical phenomena in electron-beam-generated plasmas. A great number of works are devoted to the calculation of the EDF in a uniform gas flow [1,2]. However, to our knowledge no work exists on the modeling of the EDF in a nonuniform gas flow.

This paper outlines the Monte Carlo (MC) method for the modeling of electron-beam-generated plasma in a nonuniform gas flow. The motivation for this work was provided by the problems associated with the electron beam and the laser induced fluorescence diagnostic techniques, and methods used to deposit thin films with ionized gas flows. The model described below may be useful to analyze the auroral phenomena.

II. THE MONTE CARLO ELECTRON DEGRADATION TECHNIQUE

To simulate the propagation of electrons in a nonuniform gas, the following model has been suggested. In the first stage, the monoenergetic primary electrons were incident in the simulation region, which in the beginning was empty from electrons. The region filled up gradually by electrons, and afterwards, the EDF as a function of velocity and position was produced. Since the free path was changed during the free flight, the null collision technique was employed. This technique, usually employed to simulate the motion of electrons in electric discharges [3–6], may be generalized in the case of an electron-beam-generated plasma in a nonuniform gas in an external electric and magnetic fields as follows.

The probability of scattering an electron with energy, e, in the time step τ may be written as

$$W=1-\exp\left(-\left|\int_0^\tau dt\ n_g(\vec{r}(t))\vec{v}(t)\Omega(e(t))\right|\right), \qquad (1)$$

where $n_g(\vec{r}(t))$ is the gas density in position $\vec{r}(t)$, $\Omega(e(t))$ is the total collision cross section, and $\vec{v}(t)$ is the velocity of an electron.

Let us consider for each electron not only the processes of real collisions but also for a null collision, from which an electron emerges with an unchanged velocity. Further, let us specify the cross section, $\sigma_{null}(e,\vec{r})$, for the latter process with the following expression:

$$\nu_m=n_g(\vec{r})[v\sigma_{null}(e,\vec{r})+v\Omega(e)], \qquad (2)$$

where $\nu_m=[\nu(v,\vec{r})]_{max}$ is the maximum of collision frequency. Therefore, probabilities of real $P_{real}(v,\vec{r})$ and null $P_{null}(v,\vec{r})$ collisions were determined by the relation of a frequency of the correspondent process to ν_m:

$$P_{real}(v,\vec{r})=\nu(v,\vec{r})/\nu_m,$$
$$P_{null}(v,\vec{r})=[\nu_m-\nu(v,\vec{r})]/\nu_m, \qquad (3)$$

where $\nu(v,\vec{r})=n_g(\vec{r})\Omega(e)v$ is the total frequency of a real collision.

Taking into consideration (1) and (2), the free path was found from the following expression:

$$\lambda=-(v/\nu_m)\ln(W). \qquad (4)$$

The probability formulas for real and null collisions (3) and for the free path (4) were used to avoid the calculations needed when the density changed in the free path.

The trajectory of each electron was schematized as a succession of free flights interrupted by collisions. If the scattering event was a real collision, then the type of collision for each electron would be chosen according to the distribution $\sigma_j(e)/\Omega(e)$, where $\sigma_j(e)$ is the total cross section of the jth scattering process. Elastic scattering, ionization, and excitation of electron states of molecules were considered [7].

After the type of collision had been established, the polar scattering angle of an electron was then calculated using the information on the differential cross section. The azimuthal angle was sampled according to the spatially uniform distribution. The details of calculating the scattering angles have been described in [8,9].

By monitoring the position and velocity of each electron, one could simulate the EDF as a function of velocity and position. To calculate the spatial dependencies of the excitation rates of a molecule, the simulation region was divided into cubic cells. The cell size was chosen to avoid a considerable change in the EDF for an area of a cell.

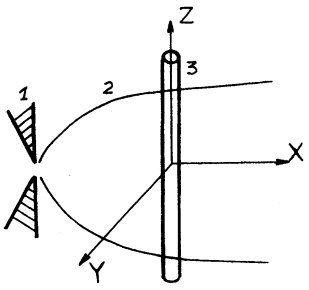

FIG. 1. A schematic diagram of the interaction of the electron beam with the jet: 1–sonic nozzle, 2–free jet expansion, 3–electron beam.

The excitation rate of the jth electron state in the center of the cell with spatial coordinates (x_i,y_i,z_i) (primary electrons were incident along the Z axis) was determined from the formula:

$$F_j(x_i,y_i,z_i) = \sum_k n_g(x_i,y_i,z_i)n(x_i,y_i,z_i,u_k,v_k,w_k)\sigma_j(e_k)e_k^{1/2},$$

where $n(x_i,y_i,z_i,u_k,v_k,w_k)$ is the distribution function of the electrons. The summation was implicated over energies of electrons in the ith cell.

Information on the distribution function of secondary electrons (arising from ionization) was obtained using the energy dependence of the number of electrons with the energies exceeding some energy, e, in a cylinder of radius R and length L around the electron beam:

$$N_{sec}(e_{min}) = \sum_i n(\eta_i,\xi_i,\mu_i,u_i,v_i,w_i), \tag{5}$$

where η_i, ξ_i, and μ_i are the spatial coordinates of ith electron, $0 \leq \eta_i^2+\xi_i^2 \leq R^2$, $-L/2 \leq \mu_i \leq L/2$, $e_{min} \leq e \leq (E_b-I)/2$; E_b is the energy of an incident electron, and I is the ionization potential of the molecule.

III. THREE-DIMENSIONAL DISTRIBUTION OF RATES OF IONIZATION AND EXCITATION OF $C\ ^3\Pi_u$ IN NITROGEN

The above model may be employed for many applications. In the present paper, we are concerned only with modeling the EDF in an axisymmetric supersonic jet of nitrogen excited by an electron beam (Fig. 1). The incident electrons were monodirectional and distributed in the (X,Y) plane ac-

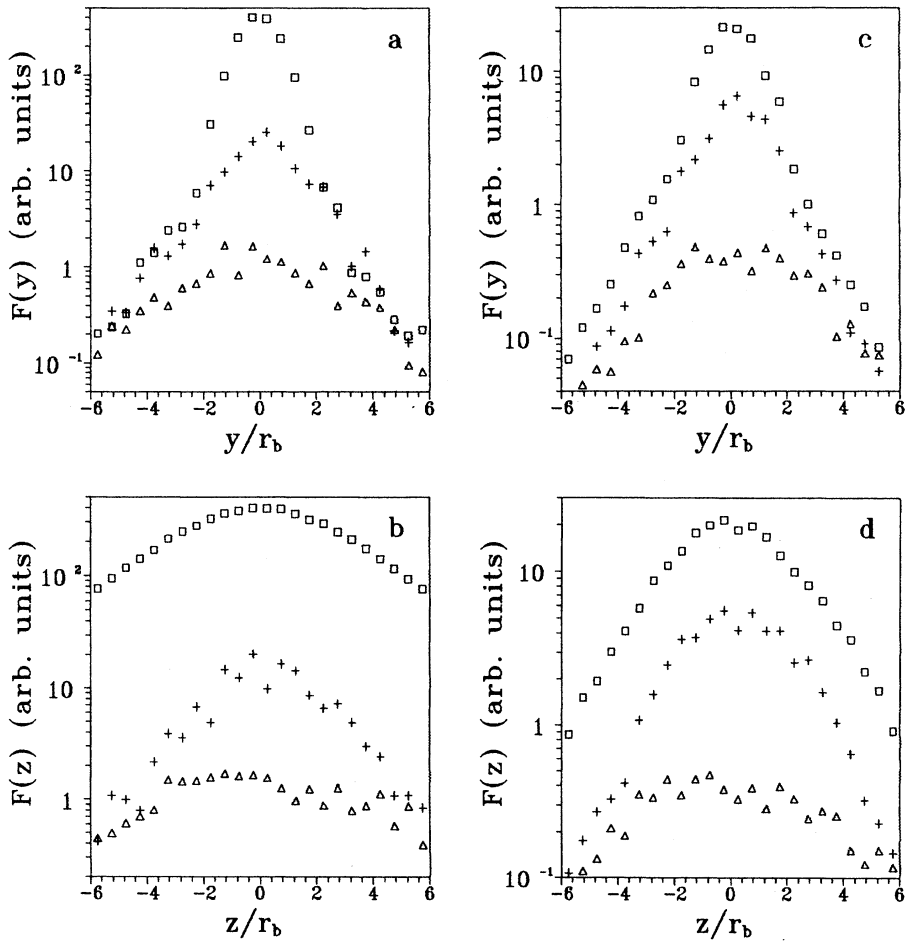

FIG. 2. Excitation rates of electron states vs the distance from the jet axis in N_2: □, $x/r_b=0$; +, $x/r_b=-2.5$; △, $x/r_b=3.5$. (a) Ionization rate along the Y axis; (b) ionization rate along the Z axis; (c) rate of excitation of state of $C\ ^3\Pi_u$ along the Y axis; (d) rate of excitation of state of $C\ ^3\Pi_u$ along the Z axis.

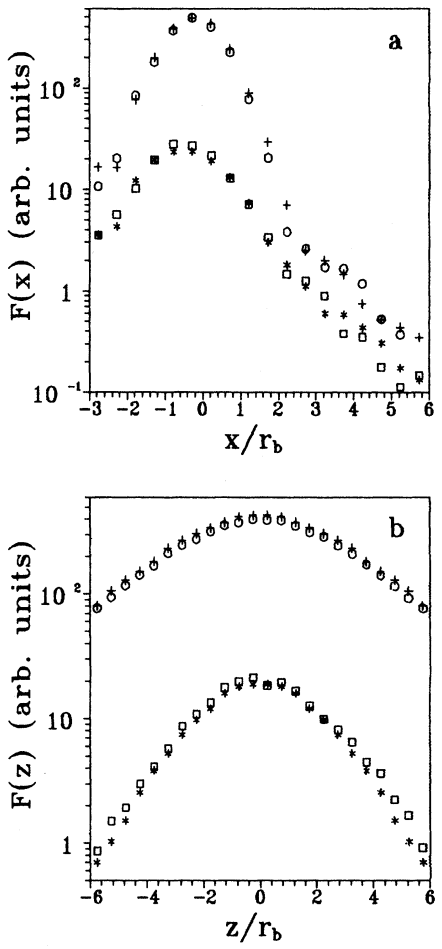

FIG. 3. Excitation rates of electron states vs the distance from the jet axis in N_2 obtained while taking into account anisotropic scattering and electron beam degradation (○, ionization rate; □, rate of excitation of state of $C\ ^3\Pi_u$) or assuming isotropic scattering (+, ionization rate; *, rate of excitation of state of $C\ ^3\Pi_u$): (a) rates of excitation along the X axis; (b) rates of excitation along the Z axis.

cording to the normal distribution (with the half-width r_b = 0.21 cm). The choice of the gas medium was conditioned by complete information on the electron scattering cross sections in nitrogen and by that the spatial distribution of density in the supersonic jet of a diatomic gas had been investigated in detail [10]. The total cross sections necessary for calculations have been discussed in [7]. The analytical approximations on the differential cross sections were taken from [11]. The spatial distribution of the density in the jet was sampled from calculations, obtained on the basis of solving the Euler equations [12]. The stagnation number density chosen was 3.6×10^{18} cm^{-3}. The diameter of the gas source was equal to r_b. The distance along the X axis from the center of the beam to the gas source was equal to $6r_b$.

The three-dimensional distribution of the ionization rate [Figs. 2(a) and 2(b)] and the excitation rate of $C\ ^3\Pi_u$ [Figs. 2(c) and 2(d)] is given as a function of position along the Y and Z axes at different distances from the center of the beam along the X axis. In the beam, the profiles of the ionization rate are determined from the result of multiplying the spatial

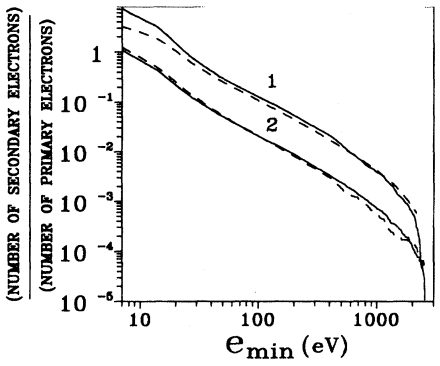

FIG. 4. The energy dependencies of normalized number of secondary electrons in N_2, in a cylinder of radius $R=5r_b$ and length $L=60r_b$ at the energy exceeding some energy value, e_{min}, obtained while taking into account anisotropic scattering and electron beam degradation (broken lines)—or assuming isotropic scattering (solid lines): 1–calculations for uniform flow, 2–calculations for the jet. The gas density at the intersection of the symmetry axes of the electron beam and the gas density in the jet were equal in a uniform flow ($n_g^{\perp}=10^{16}$ cm^{-3}).

distribution of the primary electrons and the corresponding profiles of the density. At some distance from the center of the beam, a molecule in N_2 is practically excited only by low-energy secondary electrons. A comparison between the profile of the ionization rate along the Y axis and the Z axis suggests that electrons located at a distance from the beam were distributed more uniformly in space than the primary electrons. The latter is attributed to the fact that the density decreased with increasing distance from the jet axis; therefore, secondary electrons were, for the most part, generated in the domain where the beam crossed the jet core.

The primary electrons do not contribute significantly to excitation of $C\ ^3\Pi_u$ [Figs. 2(c) and 2(d)]; therefore, in the beam, the difference between the profile of the excitation rate of $C\ ^3\Pi_u$ along the Y axis and along the Z axis is less visible than for the profiles of ionization rate. It should be stressed that at a distance from the beam the profiles of the excitation rate of $C\ ^3\Pi_u$ are similar to those of the ionization rate. Taking into consideration that the energy dependence for the cross sections of the ionization and excitation of $C\ ^3\Pi_u$ differ markedly from each other, it could expected that a similar tendency manifests itself for other excitation states of nitrogen.

Taking into account the spatial distribution of the density in a jet [10], it is possible to suggest that the electron beam degradation yields no change in the spatial and energy distribution of the electrons. In Figs. 3(a) and 3(b)], the computations of the rates of ionization and excitation of $C\ ^3\Pi_u$ along the X and Z axes were compared taking into account anisotropic scattering and electron beam degradation, or assuming isotropic scattering [13]. The figures show that the electron beam degradation as well as an anisotropic angular distribution in the scattering cross sections have little effect on the EDF.

In Fig. 4, the energy dependencies of the normalized number of secondary electrons [with the energies exceeding some energy—see Eq. (5)] to the quantity of the primary electrons in a cylinder of radius R and length L around an electron

beam are given. The figure presents the MC calculations taking into account electron beam degradation and anisotropic scattering, or assuming isotropic scattering [13]. For the jet, little difference is observed between the energy dependencies calculated using the different models of scattering. In the case of uniform flow in a high-energy range, when ionization and inelastic scattering are significant, the calculations for the different models of scattering were in a good agreement with each other. At low energies ($e \leqslant 30$ eV), when elastic scattering dominated over inelastic, the MC calculations using isotropic scattering over-estimated the number of low-energy secondary electrons. Figure 4 shows the influence of anisotropic scattering and electron beam degradation on the integral characteristics of the secondary electron distribution (when electron beam degradation was insignificant). Comparing the energy dependencies in the case of uniform and nonuniform flow shows that they have approximately the same form but the number of secondary electrons in the jet is much less than in uniform flow. The latter results from the spatial distribution of the density in the jet may cause the secondary electrons to fly away from the jet.

IV. CONCLUSIONS

This work presented the MC model of interaction of an electron beam with nonuniform gas flow. The model was utilized to determine the three-dimensional distribution of the rates of ionization and excitation of $C\ ^3\Pi_u$ in nitrogen. The results show that secondary electrons located at a distance from the beam were distributed more uniformly in space than primary electrons. This fact may be one of the reasons for the formation of spatially uniform thin films deposited from the jet excited by an electron beam. It was found that the number of secondary electrons in a finite volume was significantly less than in a nonuniform gas flow. This indicates that the ionization in a jet occurred much less efficiently than in uniform flow.

It was shown that isotropic scattering and no electron beam degradation may be considered for the modeling of the interaction of a high-energy electron beam with a low density jet. This fact is essential due to lack of information on the differential cross sections for many gases.

[1] A.E.S. Green, Radiat. Res. **64**, 119 (1975).
[2] V.P. Konovalov and E.E. Son, in *Chemical Plasma*, edited by B.M. Smirnov (Energoatomizdat, Moscow, 1987), Vol. 14, p. 194.
[3] H.R. Skullerud, Brit. J. Appl. Phys. (J. Phys. D) **1**, 1567 (1968).
[4] S.L. Lin and J.N. Bardsley, J. Chem. Phys. **66**, 435 (1977).
[5] J. Lin and G.R.G. Raju, J. Phys. D **25**, 167 (1992).
[6] A. Date, K. Kitamori, Y. Sakai, and H. Tagashira, J. Phys. D **25**, 442 (1992).
[7] V.S. Malinovsky and A.V. Vasenkov, Phys. Rev. E **50**, 4969 (1994).
[8] M.G. Heaps and A.E.S. Green, J. Appl. Phys. **45**, 3183 (1974).
[9] J.M. Berger, S.M. Seltzer, and K. Maeda, J. Atmos. Terr. Phys. **32**, 1015 (1970).
[10] H. Ashkenas and F.S. Sherman, in *Proceedings of the 4th International Symposium on Rarefied Gas Dynamics*, edited by J.N. de Leeuw (Academic, New York, 1966), Vol. 2, p. 84.
[11] C.H. Jackman and A.E.S. Green, J. Geophys. Res. **84**, 2715 (1979).
[12] P.A. Skovorodko, in *Rarefied Gas Dynamics*, edited by S.S. Kutateladze (Institute of Thermophysics, Novosibirsk, 1976), p. 91.
[13] A.V. Vasenkov and V.S. Malinovsky (unpublished).